Initial Assessment of Dye Incorporation in *Bombyx mori* Silk Biomaterials

Cindy Gu
Basis Independent Fremont
Newark, USA
cindyisawesome36@gmail.com

James Gu
Stanford University
Stanford, USA
jamesgu8@stanford.edu

***Abstract*—This study presents a preliminary and environmentally sustainable method for producing fluorescent silk by incorporating fluorescent dyes directly into the diet of *Bombyx mori* silkworms. Five dye compounds (Fluorescein Sodium, Rhodamine B, Rhodamine 101 Inner Salt, Sulforhodamine 101, and Rhodamine 110 Chloride) were administered at a 0.1% concentration (0.02 g of dye per 20 g of mulberry chow) starting at the 2nd instar. Silk cocoons formed during the 5th instar were analyzed for fluorescence, mechanical strength, and structural consistency. Rhodamine B exhibited the highest fluorescence intensity, with Rhodamine 110 Chloride having the least. Tensile strength testing showed the control group had the highest mechanical strength with Rhodamine B having the worst. Optical microscopy under ImageJ showed uniform silk structure in the control group while having inconsistency in Rhodamine 110 Chloride and Fluorescein Sodium. This method eliminates the need for post-processing while maintaining mechanical strength and stable long-term fluorescence. The resulting biocompatible silk fibers show strong potential for implantable biosensing, enabling real-time monitoring of disease markers, infections, and wound healing in regenerative medicine.**

***Keywords*—Fluorescent silk, organic dyes, Bombyx mori, biosensors, biocompatible materials, dietary dye incorporation, silk fibroin**

I. Introduction

Silk fibroin, the primary structural protein in silk, is valued for its exceptional biocompatibility, biodegradability, mechanical strength, optical clarity, and biological versatility, which allows them to be used for a plethora of biomedical uses [1]. Fluorescent silk, engineered to emit light under ultraviolet or other electromagnetic radiation, can be processed into sponges, hydrogels, 2D/3D films, fibroin mats, and fibers for various medical uses [2]. Notably, silk fibroin can maintain stable fluorescence over extended periods of time, supporting its use in biocompatible and long-term applications [3]. In tissue engineering, silk also facilitates cell adhesion and growth, making it a promising scaffold material for tissue regeneration [4].

When silk embedded with fluorescent dyes, it enables visualization of tissue growth, monitoring wound healing and tracking the distribution of drugs and cells in the body [2]. Overall, its optical properties make it valuable for monitoring biological processes and guiding tissue development [5]. Due to its porous 3D structure, it can be engineered to become scaffolds, which can be used for bone regeneration and skin tissue repair [6].

Figure 1: Examples of applications of silk used in the biomedical field [6].

Recent studies have emphasized the biomedical applications of *Bombyx mori* silk through both in vitro and in vivo analyses. In one such study, Chen et al. explored the incorporation of quercetin, a naturally fluorescent and antioxidant compound, into silk fibroin through dietary supplementation of the silkworms, followed by evaluation of growing mouse fibroblast on the resulting scaffolds [7]. Genetic modification and selective breeding of such silkworms have also improved silk yield, purity, and structural properties as well to allow scientists to fabricate scaffolds that most similarly match natural tissues [8].

Another study uses in vitro tests on testing the biocompatibility of knitted silk fibroin scaffolds made from non-mulberry silk fibroin, and investigating cell growth and regeneration from these tissue-engineered biomaterials [9]. Their study focuses on the clinical challenge of rotator cuff tendon tears as Musson et al. investigated Spidrex®, a new scaffold made from non-mulberry silk fibroin to see if it could support tendon repair [9].

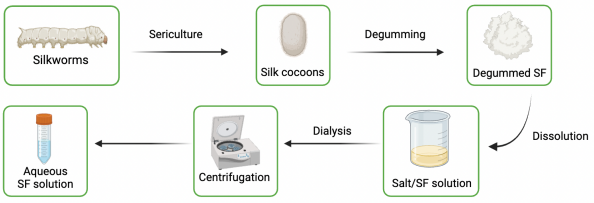

Figure 2: Process of degumming a silk cocoon from a silkworm into an Aqueous Silk Fibroin solution. Created using Biorender.com

Through using in vivo tests on investigated self-assembling silk fibroin hydrogels from *Bombyx mori* for promoting tissue

repair, Gorenkova et al. inspects the biocompatibility and interaction in experimental strokes on rats [10]. Immunofluorescence staining showed the hydrogel interacted with but did not disrupt with the surrounding astrocytes, and the hydrogel structure provided a supportive microenvironment for cellular proliferation as a minimally invasive biomaterial for enhancing post-stroke brain repair [10]. Yigit et al. found that silk fibroin, tested for mutagenicity, genotoxicity, and systematic toxicity through micronucleus assays and rat feeding studies, showed no DNA damage or toxic effects even at high doses, supporting its safety for biomedical use [11].

In the study from Pang et al., researchers fabricated fluorescent silk fibroin nanofibers using electrospinning with three dyes, Fluorescein Sodium, Rhodamine B, and Acridine orange [12]. Structural analyses showed that the dyes did not alter the silk fibroin's structure, and thermal degradation consistently began around 250 °C [12].

Additionally, Yamane et al. studied the structural organization of *Bombyx mori* silk fibroin in its unspun silk, and simulated three dipeptides, Ac-Gly-NHMe, Ac-Ala-NHMe, and Ac-SerNHMe in water to understand the crystalline regions of fibroin [13]. This supported the idea that silk fibroin in its unspun form is made of repeated β-turns structures, and found that some β-turns stayed stable while others were looser [13].

This study builds upon prior research exploring environmentally friendly methods of producing modified silk using silkworms. Xiong et al. developed a safe and innovative technique using red carbon dots extracted from mulberry leaves to induce fluorescence in silk [14].

Although prior studies have advanced the development of fluorescent silk, key research gaps remain. However, there has been no comprehensive study comparing different fluorescent dyes and their effects on both silk properties and silkworm health. Additionally, the physiological response of silkworms to each dye is assessed by observing body coloration and fluorescence under visible and 365 nm ultraviolet (UV) light. Lastly, this study compares two environmentally sustainable delivery methods, dyed mulberry leaves and mulberry chow, to determine the most effective approach for incorporating fluorescent dyes into silkworm diet.

II. Methodology

A. Different Types of Fluorescent Dyes

The dye materials used in this experiment were organic, non-nanomaterial dyes, including Rhodamine 101 Inner Salt, Rhodamine 123, Rhodamine 6G, Rhodamine B, Sulforhodamine 101, Acridine Orange, and Fluorescein Sodium (Sigma Aldrich).

B. Raising Silkworms

Silkworms were raised at 24–29 °C and initially fed mulberry leaves before transitioning to chow for dye incorporation. The control group received plain chow, while experimental groups were fed chow containing 0.1% dye (0.02 g per 20 g chow, ~1 mg/g feed). At the fifth instar, larvae consumed 3–5 g daily, ingesting about 3–5 mg of dye each day.

C. Mechanical Properties

To evaluate the mechanical properties of the silk, tensile strength was measured using a spring scale to record the maximum load each silk strip (3 × 2 cm) could withstand before failure. Samples were looped around the scale hook, pulled until lock, and tested ten times per group to ensure consistency and allow comparison across dye treatments. This repeated testing reduced experimental error and improved reliability of the data. The results provided a quantitative basis for evaluating how each dye affected the structural integrity of the silk..

III. Results and Discussion

The lifecycle progression of *Bombyx mori* is critical to understanding when dye exposure is most effective. As illustrated in Fig. 3, the full lifecycle spans approximately 45-50 days, beginning with the egg stage (Fig. 3A). By day 5, the larvae enter the 1st instar (Fig. 3B), feeding on the edges of mulberry leaves. Around day 9 (Fig. 3C), they molt into the 2nd instar and were divided into equal groups and placed in separate enclosures to receive different fluorescent dye treatments. By day 30, they reach the 4th to 5th instar stage (Fig. 3D). Fig. 3E shows a completed cocoon, where the silkworm pupates until it emerges as a moth around day 50 (Fig. 3F).

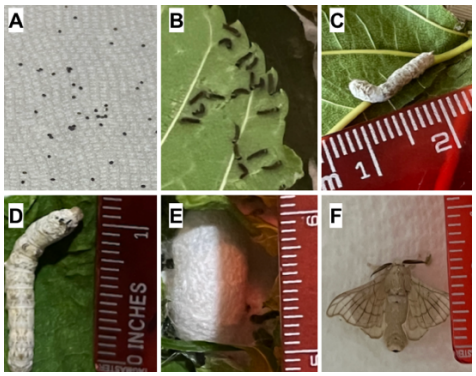

Figure 3: Silkworm life cycle. A) silkworm eggs; B) silkworm on day 5 (1st instar); C) silkworm on day 9 (2nd instar); D) silkworm on day 30 (4th and 5th instar); E) silkworm cocoon day 30; and F) silk moth

A total of 200 silkworms were divided into six dye-fed groups of 33 and one control group (with 2 extra worms added for balance). All groups received standard chow during the first two instars, after which experimental groups were fed dye-supplemented chow while controls remained on plain chow. From the third instar onward, five silkworms per group were randomly selected daily to asses movement activity and body coloration.

To assess dye fluorescence, Fig. 4 presents organic fluorescent dyes under both room and UV lighting. In Fig. 4A, the dyes are shown under room lighting, where each exjibits strong color saturation. Fig 4B presents the same dyes under 365 nm UV light, where all mixtures demonstrate high fluorescence, confimring their suitability for dietary incorporation. This also proves how fluorescent dyes are absorbed through the silkworm body, through the digestive system and incorporated into their coloration and silk glands.

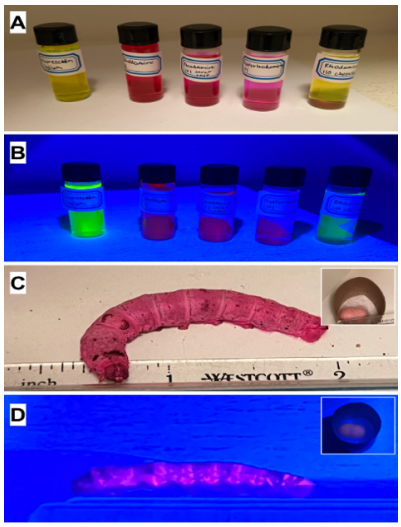

Figure 4: A-B) Fluorescent mixture under room lighting on top and UV lighting on bottom (Fluorescein Sodium, Rhodamine B, Rhodamine 101 Inner Salt, Sulforhodamine 101, Rhodamine 110 Chloride); C) Example of dyed silkworm and its cocoon of Rhodamine B dye under room light; and D) Example of Rhodamine B dyed silkworm and its cocoon under UV light

Expanding on these results, Fig. 5 illustrates how the dyes affected the silkworms' appearance under room and UV lighting. The silkworms that ingested dyes with a pink hue, specifically Sulforhodamine 101, Rhodamine 101 Inner Salt, and Rhodamine B, exhibited the highest fluorescence under UV light (Figs. 4C-E), indicating effective absorption through the silkworms' digestive system. In contrast, Fluorescein Sodium and Rhodamine 110 Chloride produced strong yellow fluorescence in solution but failed to generate visible fluorescence in the silkworms themselves. As shown in Figs. 5A and 5B, these silkworms displayed no change under UV light.

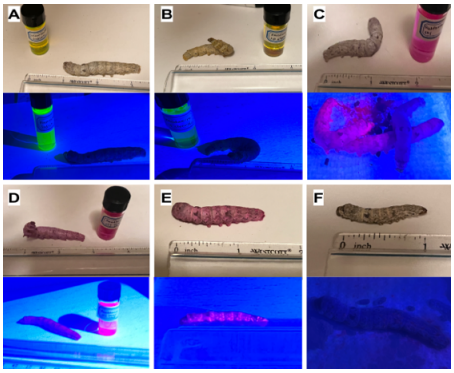

Figure 5: A-F) Different dyed silkworm under room lighting on top and under UV light (Fluorescein Sodium, Rhodamine 110 Chloride, Sulforhodamine 101, Rhodamine 101 Inner Salt, Rhodamine B, Control Group)

The impact of dye ingestion on silk is further detailed in Fig. 6, which shows silk scaffolds under both lighting conditions. Under room lighting, Rhodamine B (Fig, 6A) and Rhodamine 101 Inner Salt (Fig. 6E) exhibited the most intense coloration. These were followed by Rhodamine 110 Chloride (Fig. 6B) with an orange hue, Sulforhodamine 101 (Fig. 6C0 with a purple hue, Fluorescein Sodium (Fig. 6D) with a green hue, and lastly the control group (Fig. 6F), which showed no coloration.

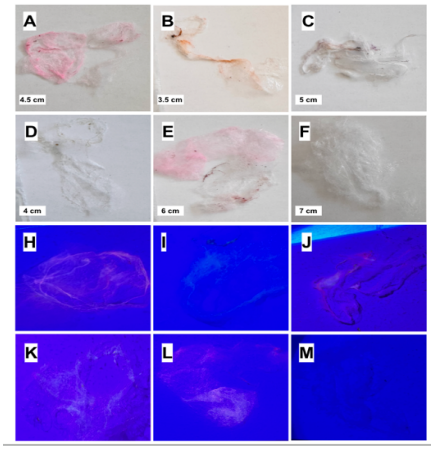

Figure 6: A-F) Silkworm silk under room light with different dye with the white bar indicating the length of each silk scaffold (Rhodamine B (pink), Rhodamine 110 Chloride (orange), Sulforhodamine 101 (purple), Fluorescein Sodium (green), Rhodamine 101 Inner Salt (pink), and Control Group); and H-M) Silk corresponding to A-F under 365 nm UV light

To analyze how dye incorporation affects fiber structure, Fig. 7 presents microscopic images of silk scaffolds under 4x objective magnification to evaluate the effects of dye incorporation on silk uniformity and mechanical properties. The control group (Fig. 7F) shows a highly uniform fiber alignment, showing the silk retains its native structure. In contrast, Sulforhodamine 101 (Fig. 7A), Rhodamine B (Fig. 7D), and Rhodamine 101 Inner Salt (Fig. 7E) exhibit moderate alignment, but still less uniform than the control. Rhodamine 110 Chloride (Fig. 7B) and Fluorescein Sodium (Fig. 7C) are disorganized.

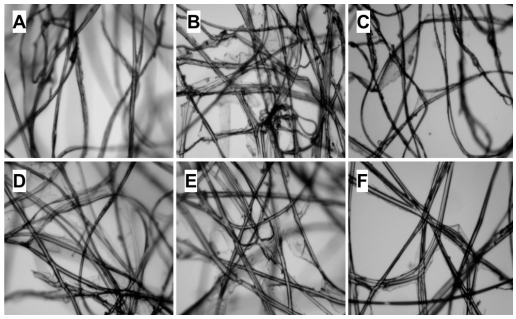

Figure 7: Different types of silk under microscope. A) Example of Sulforhodamine 101 silk; B) Example of Rhodamine 110 Chloride silk; C) Example of Fluorescein Sodium silk; D) Example of Rhodamine B silk; E) Rhodamine 101 Inner Salt silk; F) Example of Control Group silk without the addition of dyes

To quantify structural effects, Fig. 8 presents tensile strength measurements. Each sample was tested 10 times on a spring scale, with maximum force (N) recorded. The control group showed the highest strength (7.27±0.56), confirming that undyed silk retains native integrity. Sulforhodamine 101 (5.52±0.52) and Rhodamine 101 Inner Salt (4.21±0.37) maintained relatively high values, suggesting minimal disruption to silk proteins. Rhodamine 110 Chloride (3.26 ± 0.39), Fluorescein Sodium (2.56±0.38), and Rhodamine B ((3.16±0.29) had reduced strength.

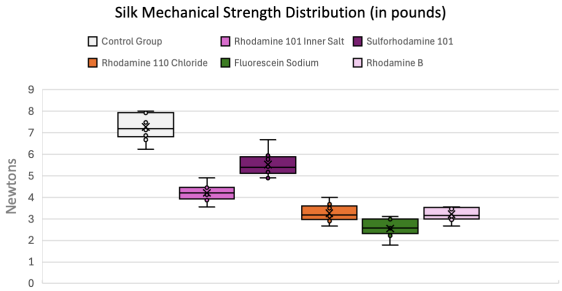

Figure 8: Whisker plot of the tensile strength of each silk scaffold in Newtons, corresponding to their color (Control Group, Rhodamine 101 Inner Salt, Sulforhodamine 101, Rhodamine 110 Chloride, Fluorescein Sodium, and Rhodamine B)

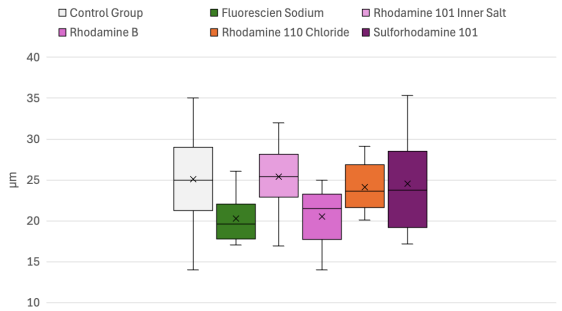

Figure 9: Box whisker plot of each silk strand diameters (in µm) of each fluorescent dye group, corresponding to their color (Control Group, Fluorescein Sodium, Rh 101 Inner Salt, Rh B, Rh 110 Chloride, Sulforhodamine 101)

Fiber morphology was evaluated by measuring strand diameters from micrographs (Fig. 7), with group-level means summarized in Fig. 9. Scale bars were calibrated in micrometers (µm), and each group were averaged. The control (25.10 µm) and Rhodamine 101 Inner Salt (25.40 µm) groups had the largest diameters, indicating minimal structural degradation. In contrast, Fluorescein Sodium (20.27 µm), Rhodamine B (20.50 µm), and Rhodamine 110 Chloride (20.50 µm) showed smaller diameters, consistent with reduced strength. Statistical analysis confirmed a significant reduction for Fluorescein Sodium ($p = 0.039$), while Rhodamine B (0.056), Rhodamine 110 Chloride (0.661), Sulforhodamine 101 (0.839), and Rhodamine 101 Inner Salt (0.900) were not significantly different from controls.

IV. Conclusion

The five organic fluorescent dyes evaluated in this study were chosen for their ability to produce stable, high fluorescence. Fluorescent silk scaffolds were then produced and checked for fluorescence intensity under a 365 nm UV light under visualization. The results indicated that Rhodamine B had the highest fluorescence intensity under 365 nm UV light, followed by Sulforhodamine 101, Fluorescein Sodium, Rhodamine 101 Inner Salt, Rhodamine 110 Chloride, and finally control group having the lowest fluorescence intensity. Quantitative fiber analysis showed that groups like Rhodamine 101 Inner Salt maintained larger strand diameters (25.40 µm) and more consistent morphology, while certain dyes such as Fluorescein Sodium (20.27 µm) reduced strand size, correlating with lower mechanical performance (2.56±0.38).

Overall, these findings demonstrate that dietary dye incorporation is a practical and sustainable approach to producing fluorescent silk, establishing clear relationships between dye chemistry, fiber structure, and mechanical behavior. Future work also includes adding a reference sheet to compare current silk scaffolds with a reference sheet to identify the data points of each fluorescence intensity.

References

[1] D. W. Kim *et al.*, "Novel fabrication of fluorescent silk utilized in biotechnological and medical applications," *Biomaterials*, vol. 70, pp. 48–56, Nov. 2015, doi: https://doi.org/10.1016/j.biomaterials.2015.08.025.

[2] Z.-F. Wu, Z.-N. Sun, and H.-M. Xiong, "Fluorescent Silk Obtained by Feeding Silkworms with Fluorescent Materials," Chin. J. Chem, vol. 41, pp. 2035–2046, 2023, doi: https://doi.org/10.1002/cjoc.202300043.

[3] K. Shimizu, "Genetic engineered color silk: Fabrication of a photonics material throuan gh a bioassisted technology," *Bioinspir. Biomim.,* 2018. [Online]. Available: https://pubmed.ncbi.nlm.nih.gov/29620530/.

[4] C. Lujerdean, G.-M. Baci, A.-A. Cucu, and D. S. Dezmirean, "The contribution of silk fibroin in biomedical engineering," *Insects*, vol. 13, no. 3, p. 286, Mar. 2022, doi: 10.3390/insects13030286.

[5] H. Xu and D. A. O'Brochta, "Advanced technologies for genetically manipulating the silkworm *Bombyx mori*, a model lepidopteran insect," *Proc. R. Soc. B Biol. Sci.*, vol. 282, no. 1810, p. 20150487, Jul. 2015, doi: https://doi.org/10.1098/rspb.2015.0487.

[6] T. P. Nguyen *et al.*, "Silk Fibroin-Based Biomaterials for Biomedical Applications: A Review," *Polymers*, vol. 11, no. 12, p. 1933, Nov. 2019, doi: https://doi.org/10.3390/polym11121933.

[7] W. Chen, G. Fu, Y. Zhong, Y. Liu, H. Yan, and F. Chen, "Antioxidant High-Fluorescent Silkworm Silk Development Based on Quercetin-Induced Luminescence," ACS Biomaterials Science & Engineering, vol. 11, no. 3, pp. 1402–1416, Feb. 2025, doi: https://doi.org/10.1021/acsbiomaterials.4c02400.

[8] G. De Giorgio et al., "Silk Fibroin Materials: Biomedical Applications and Perspectives," Bioengineering, vol. 11, no. 2, p. 167, Feb. 2024, doi: https://doi.org/10.3390/bioengineering11020167.

[9] D. S. Musson et al., "In Vitro Evaluation of a Novel Non-Mulberry Silk Scaffold for Use in Tendon Regeneration," Tissue Engineering. Part A, vol. 21, no. 9–10, pp. 1539–1551, May 2015, doi: https://doi.org/10.1089/ten.tea.2014.0128.

[10] N. Gorenkova, Ibrahim Osama, F. P. Seib, and H. V. O. Carswell, "In Vivo Evaluation of Engineered Self-Assembling Silk Fibroin Hydrogels after Intracerebral Injection in a Rat Stroke Model," ACS Biomaterials Science & Engineering, vol. 5, no. 2, pp. 859–869, Nov. 2018, doi: https://doi.org/10.1021/acsbiomaterials.8b01024.

[11] S. Yigit et al., "Toxicological assessment and food allergy of silk fibroin derived from *Bombyx mori* cocoons," Food and Chemical Toxicology, vol. 151, p. 112117, May 2021, doi: https://doi.org/10.1016/j.fct.2021.112117.

[12] L. Pang, J. Ming, F. Pan, and X. Ning, "Fabrication of Silk Fibroin Fluorescent Nanofibers via Electrospinning," Polymers, vol. 11, no. 6, pp. 986–986, Jun. 2019, doi: https://doi.org/10.3390/polym11060986.

[13] T. Yamane, Kôsuke Umemura, and T. Asakura, "The Structural Characteristics of *Bombyx mori* Silk Fibroin before Spinning As Studied with Molecular Dynamics Simulation," Macromolecules, vol. 35, no. 23, pp. 8831–8838, Oct. 2002, doi: https://doi.org/10.1021/ma0209390.

[14] J. Liu, T. Kong, and H. Xiong, "Mulberry-leaves-derived red-emissive carbon dots for feeding silkworms to produce brightly fluorescent silk," *Adv. Mater.*, p. 2200152, Mar. 2022, doi: 10.1002/adma.202200152.